Collective dynamics of liquid aluminum probed by inelastic x-ray scattering

T. Scopigno,[1] U. Balucani,[2] G. Ruocco,[3] and F. Sette[4]
[1]*Dipartimento di Fisica and INFM, Universitá di Trento, I-38100 Povo, Italy*
[2]*Istituto di Elettronica Quantistica CNR, I-50127 Firenze, Italy*
[3]*Dipartimento di Fisica and INFM, Universitá di L'Aquila, I-67100 L'Aquila, Italy*
[4]*European Synchrotron Radiation Facility, Boîte Postale 220, F-38043 Grenoble Cedex, France*
(Received 17 July 2000; revised manuscript received 11 October 2000; published 27 December 2000)

An inelastic x-ray scattering experiment has been performed in liquid aluminum for the purpose of studying the collective excitations at wave vectors below the first sharp diffraction peak. The high instrumental resolution (up to 1.5 meV) allows an accurate investigation of the dynamical processes in this liquid metal on the basis of a generalized hydrodynamics framework. The outcoming results confirm the presence of a viscosity relaxation scenario ruled by a two-time-scale mechanism, as recently found in liquid lithium.

DOI: 10.1103/PhysRevE.63.011210 PACS number(s): 61.10.Eq, 67.40.Fd, 67.55.Jd, 63.50.+x

I. INTRODUCTION

In the past two decades, the dynamical properties of liquid metals have been widely investigated aiming at the comprehension of the role of the mechanisms underlying the atomic motions at the microscopic level. In particular, in the special case of alkali metals, it is known that well-defined oscillatory modes persist well outside the strict hydrodynamic region, down to wavelengths of a few interparticle distances, making these systems an ideal workbench to test the different theoretical approaches developed so far for the microdynamics of the liquid state. From the experimental point of view, it is worth mentioning the pioneering inelastic neutron scattering (INS) experiment by Copley and Rowe [1] in liquid rubidium, while more recently much experimental effort in performing more and more accurate experiments has been made: INS investigations have been devoted to liquid cesium [2], sodium [3], lithium [4], potassium [5], and again rubidium [6]. Many numerical studies have been reported on the same systems, allowing us to overcome such experimental restrictions as the $(Q-E)$ accessible region when dealing with the collective properties (with the density fluctuation spectra), and the simultaneous presence of coherent and incoherent contributions in the INS signal, which was the paramount experimental technique in this field up to a few years ago. Moreover, numerical techniques allow us to access a wider set of correlation functions while the inelastic scattering experiment basically probes the density autocorrelation function.

On the theoretical side, thanks to the development of such tools as the memory function formalism, the relaxation concept, and the kinetic theory [7,8], a framework has been established in order to describe the behavior of the aforementioned correlation functions. In this respect, among the most important tasks, there is the idea that the decay of the density autocorrelation function occurs over different time scales. In particular, a first mechanism is related to the coupling of the density and the temperature modes (thermal relaxation), while a second process involves the stress correlation function (viscosity relaxation). The latter mechanism proceeds through two different relaxation channels, active over different time scales: a first rapid decay, which has been ascribed to cage effects due to microscopic interaction of each atom and the cage of its neighboring atoms, followed by a slower process related to the long-time rearrangements that drives the glass transition in those systems that are capable of supercooling. This structural relaxation process has been widely studied in the mode-coupling formalism and recently remarkable efforts have been developed to set up self-consistent approaches [9]. This theoretical framework has been tested on a number of numerical studies (see, for example, [10] and references therein). Indeed, the line shape of the density correlation spectra extracted by INS [in those systems where it is allowed in the significant $(Q-E)$ region] did not allow us to discriminate between different models including all the relevant relaxation processes at the microscopic level [2].

In the recent past, the development of new synchrotron radiation facilities opened the possibility of using x rays to measure the $S(Q,\omega)$ (which is proportional to the scattered intensity) in the nonhydrodynamic region; in this case, the photon speed is obviously much larger than the excitations velocity, and no kinematic restriction occurs. Moreover, in a monatomic system, the inelastic x-ray scattering (IXS) cross section is purely coherent and so it is directly associated with the dynamic structure factor.

Recently, an accurate IXS study on liquid lithium allowed us to detect experimentally the presence of the relaxation scenario predicted by theory on this prototypical alkali metal [11]. In particular, the data have been analyzed within a generalized hydrodynamic approach [10,12] and, following a memory function formalism [7], it has been possible to detect the presence of two relaxation processes (additional to the thermal process resulting from the coupling of density and temperature variables) affecting the dynamics of the systems in the mesoscopic wave-vector region [13]. This result, obtained with a phenomenological ansatz for the memory function originally proposed in a theoretical work by Levesque *et al.* [8], has been deeply discussed, pointing out the physical origin of such dynamical processes [14].

Although alkali metals are commonly referred to as the ''paradigm of simple liquids,'' other liquid metals always exhibit the characteristic structural and dynamical features that can be interpreted within the elementary approaches

typically utilized when dealing with Lennard-Jones or alkali-metal interatomic potentials [15,16]. A remarkable example is provided by liquid aluminum. Several theoretical [17] and numerical [18] works have been reported on this system. In fact, the basic common features of simple liquids, such as the presence of collective excitations in the coherent dynamic structure factor below Q_m and the positive dispersion of the sound speed associated with them, have been extensively studied in this liquid. On the other hand, in this Q region no experimental data have been reported to provide a real test and/or comparison of collective dynamics. Indeed, in liquid Al, the high value of the isothermal sound speed $c_0 \sim 4700$ m/s prevents, due to kinematic reasons, a study of the collective dynamics by INS: below Q_m, the available energy transfer is too limited to investigate the acoustic excitations properties. Accurate INS data have instead been reported at higher wave vectors where, however, the single-particle response is mainly probed (see, for example, Ref. [19]).

In this work, we present the study of the coherent dynamic structure factor, $S(Q,\omega)$, of liquid aluminum ($T = 1000$ K) by inelastic x-ray scattering, in a wave-vector region, $0.05Q_m \leqslant Q \leqslant 0.5Q_m$, of crucial importance as far as the dynamical features of the collective motion are concerned.

II. EXPERIMENT

Our IXS experiment has been carried out at the high-resolution beamline ID16 of the European Synchrotron Radiation Facility (Grenoble, France). The incident beam is obtained by a backscattering monochromator operating at the (*hhh*) silicon reflections, with $h = 9,11$. The scattered photons are collected by spherically bended Si crystal analyzers working at the same (*hhh*) reflections. The total energy resolution function, measured from the elastic scattering by a Plexiglas sample, has a full width at half maximum (FWHM) of 3 meV for $h = 9$ and 1.5 meV for $h = 11$: this higher-resolution configuration has been used at $Q = 1$ and 2 nm^{-1}, where the width of the spectral features starts to be comparable to the resolution width at $h = 9$. The wave vector transferred in the scattering process, $Q = 2k_i \sin(\theta_s/2)$ (with k_i the wave vector of the incident photon and θ_s the scattering angle) is selected between 1 nm^{-1} and 14 nm^{-1} by rotating a 7-m-long analyzer arm in the horizontal scattering plane. The total (FWHM) Q resolution has been set to 0.4 nm^{-1}. A five-analyzers bench was used to collect simultaneously five different Q values, determined by a constant angular offset of 1.5° between neighboring analyzers. Energy scans have been performed by varying the temperature of the monochromator with respect to that of the analyzer crystals. Each scan took about 180 min, and each spectrum at a given Q was obtained from the average of two to eight scans, depending on the values of h and Q. The data have been normalized to the intensity of the incident beam. The liquid aluminum sample (0.999% purity) has been kept in an Al_2O_3 container with optically polished single-crystal sapphire windows (0.25 mm thick). The sample length, which for an IXS scattering experiment is optimal if coincident with the absorption length, has been set to 1.0 mm in order to be nearly optimized for both $h = 9,11$ energies (21 747 and 17 794 eV, respectively). The cell was then placed inside a molybdenum oven in thermal contact with a tantalum foil heated by the dissipation of about 100 W of power. The whole environment has been kept in a 10^{-7} mbar dynamic vacuum.

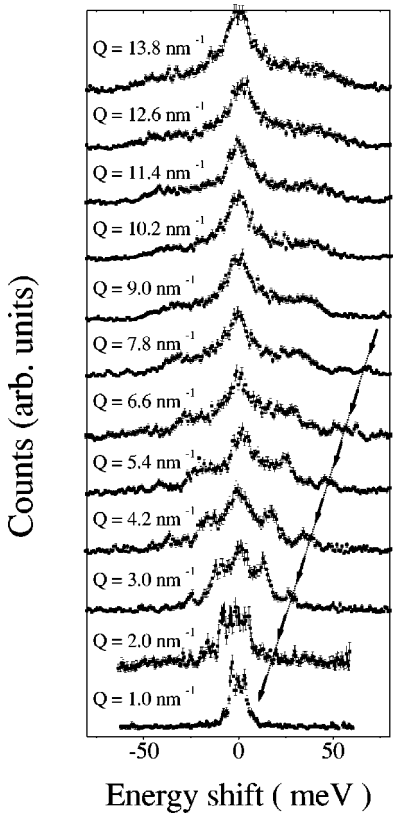

FIG. 1. IXS spectra of liquid aluminum at the indicated wave vectors. The instrumental resolution is $\Delta E = 1.5$ meV at $Q = 1$ and 2 nm^{-1} and $\Delta E = 3.0$ meV elsewhere. The total integration time is about 500 s for each point.

The IXS spectra $I(Q,\omega)$, collected at fixed Q as functions of the exchanged energy, are reported in Fig. 1. As $Q_m = 25\ \mathrm{nm}^{-1}$, from the raw spectra we can observe the relevant region of dispersion of the acoustic mode. Initially, the frequency of the inelastic peaks increases linearly with Q. Despite an increase with Q of their width, the modes are recognizable even at the highest wave vectors explored in the experiment. As expected, the ratio between the energy loss/gain sides of the spectra is ruled out by the detailed balance condition. The quasielastic portion of the spectra, associated to some still unrelaxed damping mechanism, shows a linewidth that increases with Q, as the characteristic time scale of such a process suddenly decreases at decreasing the dominant wavelength of the observed density fluctuation.

At the lower Q values, a non-negligible contribution coming from the empty container scattering is clearly visible (arrows in Fig. 1). This feature basically stems from the inelastic scattering of the sapphire windows. As the longitudinal phonon velocity in Al_2O_3 is more than 10 000 m/s, this ''spurious'' contribution is beyond the energy region relevant for liquid Al and does not significantly affect the main spectral features of interest. However, for an accurate quan-

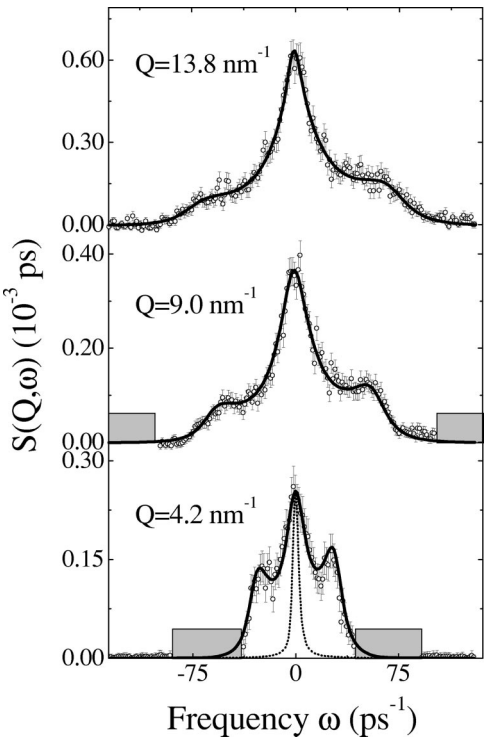

FIG. 2. Selected examples of the fitting procedure. Open circles with the error bars are the IXS data; the full lines are the best fit to the data. The shadow boxes indicate the energy windows that have been cut off in the fitting session. The resolution function is also reported (dotted line).

titative assessment of the spectral shape at the lower Q values, in the analysis we have excluded the undesired portions around the Al_2O_3 phonons by cutting off the two corresponding energy ranges (shadowed areas in Fig. 2).

III. DATA ANALYSIS

The spectra $S(Q,\omega)$ have been described within the framework of the generalized Langevin equation for the density correlator $\phi(Q,t)=\langle \rho_Q(t)\rho_{-Q}(0)\rangle/\langle|\rho_Q(t)|^2\rangle$:

$$\ddot{\phi}(Q,t)+\omega_0^2(Q)\phi(Q,t)+\int_0^t M(Q,t-t')\dot{\phi}(Q,t')dt'=0,$$

where

$$\omega_0^2(Q)=[k_BT/mS(Q)]Q^2=[c_0(Q)Q]^2. \tag{1}$$

In these equations, m is the atomic mass, $S(Q)$ the static structure factor, $c_0(Q)$ the Q-dependent isothermal sound velocity, and $M(Q,t)$ the full memory function. Recalling that the Fourier transform of $\phi(Q,t)$ is $S(Q,\omega)/S(Q)$, and introducing the Fourier-Laplace transform of the memory function as $M(Q,\omega)=M''(Q,\omega)+iM'(Q,\omega)$, the previous expression becomes

$$\frac{S(Q,\omega)}{S(Q)}=\frac{\pi^{-1}\omega_0^2(Q)M'(Q,\omega)}{[\omega^2-\omega_0^2+\omega M''(Q,\omega)]^2+[\omega M'(Q,\omega)]^2}. \tag{2}$$

All the details of the microscopic interactions are now embodied in the memory function $M(Q,t)$. For the latter, we have allowed a two-time relaxation mechanism of nonthermal contributions by assuming that

$$M(Q,t)=(\gamma-1)\omega_0^2(Q)e^{-D_TQ^2t}+\Delta^2(Q)[A(Q)e^{-t/\tau_\alpha(Q)}+[1-A(Q)]e^{-t/\tau_\mu(Q)}], \tag{3}$$

where τ's, Δ^2, and A are the time scales, the total viscous strength, and the relative weight of the two processes, respectively. In Eq. (3), the first term comes from the coupling between density and thermal fluctuations ($\gamma=C_P/C_V$ is the specific-heat ratio and $D_T=\kappa/nC_V$ the thermal diffusivity), while the other two contributions describe the relaxation of purely viscous decay channels. As is well known, for the latter the familiar viscoelastic model assumes a single exponential decay. However, as already found in liquid lithium [13,14], this simple ansatz is not accurate enough to reproduce the details of the IXS spectra in liquid Al.

Before any discussion of the fitting procedure, we recall that the actual scattered intensity is proportional to the convolution between the experimental resolution function and the true (quantum-mechanical) dynamic structure factor $S_q(Q,\omega)$, affected by the detailed balance condition. To account for the latter, we have used the following approximation:

$$S_q(Q,\omega)=\beta\hbar\omega/(1-e^{-\beta\omega})S(Q,\omega), \tag{4}$$

which connects $S_q(Q,\omega)$ with its classical counterpart $S(Q,\omega)$.

Summing up, we used Eqs. (2) and (3) as a model function. We modified it according to Eq. (4) and, finally, we folded it with the experimental resolution. The result has been utilized as a fitting function $F(Q,\omega)$ for the scattered intensity $I(Q,\omega)$:

$$F(Q,\omega)=E(Q)\int R(\omega-\omega')S_q(Q,\omega')d\omega', \tag{5}$$

where the constant $E(Q)$ depends on each analyzer efficiency and on the atomic form factor. The parameters $S(Q)$ and $\omega_0^2(Q)$ are related by Eq. (1), so that the most obvious procedure would be to put the data on an absolute scale estimating $S(Q)$ in a fitting-independent way and to fix $\omega_0^2(Q)$ accordingly. Consequently, (i) the constant $E(Q)$ in Eq. (5) would be $E(Q)=1$, (ii) the only free fitting parameters would be the relaxation times and strengths of the viscous channels [for the thermal quantities $D_T(Q)$ and $\gamma(Q)$, we have utilized their $Q\to0$ value]. This method has been successfully applied in the lithium experiment, where the $S(Q)$ has been estimated from the raw spectra utilizing the first two sum rules corrected for finite resolution effects [14]. In the present case, instead, due to the presence of empty cell contributions in the tails of the scattered intensity, an estimate of the spectral moment would not be reliable. For this reason, we have chosen to leave $E(Q)$ and $\omega_0^2(Q)$ as free

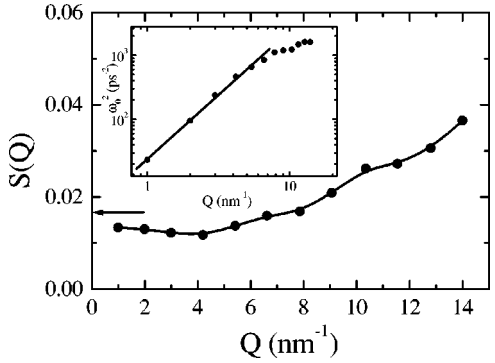

FIG. 3. Inset: $\omega_0^2(Q)$ as free fitting parameter. The full line is the expected power 2 behavior. In the main figure, values of $S(Q)$ deduced by the previously determined $\omega_0^2(Q)$ as $S(Q) = KTQ^2/m\omega_0^2(Q)$. The arrow indicates the thermodynamic value of $S(0)$ by compressibility data.

parameters. The best-fitted value of the latter quantity has therefore been used to calculate $S(Q)$, putting the data on an absolute scale.

Some examples of the quality of the described fitting procedure are reported in Fig. 2, while the reliability of the normalization method is illustrated in Fig. 3, where the inset reports on a log scale the parameter $\omega_0^2(Q)$. The value of $S(Q)$ at small Q is seen to be in fair agreement with the thermodynamic value (arrow) [18].

In Fig. 4, the relative weight $A(Q) = \Delta_\alpha^2(Q)/[\Delta_\alpha^2(Q) + \Delta_\mu^2(Q)]$ is shown. Compared to the liquid lithium, $A(Q)$ in liquid Al appears to have a faster decrease with the wave vector, indicating a somehow smaller role of slow features at finite wave vectors in this system.

In Fig. 5, we report for both mechanisms the relaxation times and, in the inset, the quantity $\omega_l(Q)\tau(Q)$, where $\omega_l(Q)$ is the maximum of the longitudinal current correlation spectra.

The characteristic time τ_μ of the microscopic process moderately decreases with Q, while the much longer τ_α is almost constant, except for an abrupt initial decrease at very

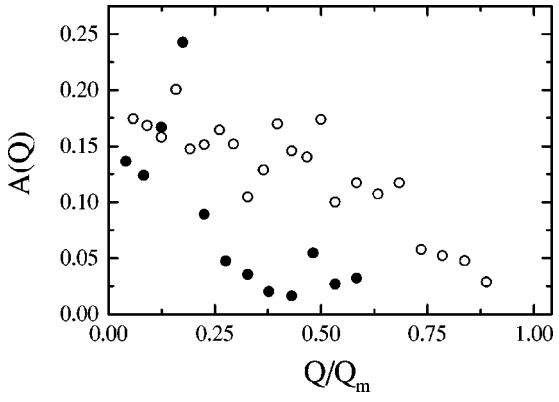

FIG. 4. Ratio $A(Q)$ between the slow and the total relaxation strength. Full dots (●) lithium, open dots (○) aluminum, both slightly above the melting point. In order to compare the two systems, the exchanged wave vector has been normalized to the static structure factor maximum.

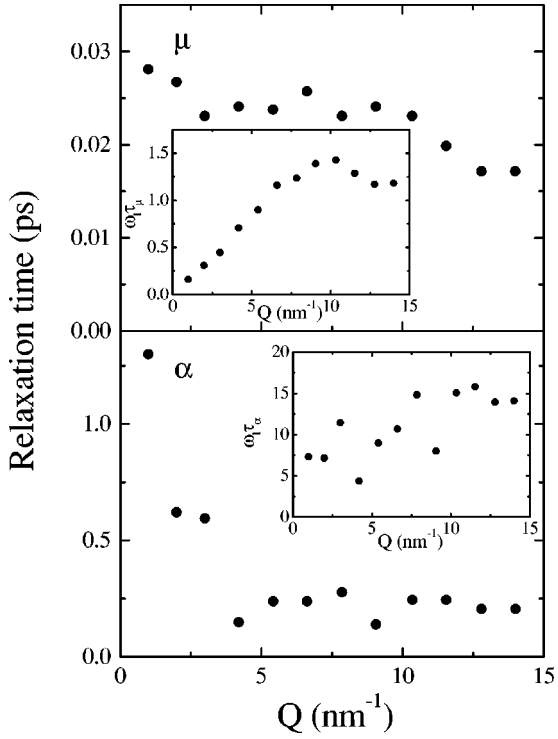

FIG. 5. Relaxation times and $\omega_l(Q)\tau(Q)$ values determined by the fitting.

low Q, which may possibly be due to finite resolution effects. From some algebraic manipulations of Eqs. (2) and (3), it is possible to infer the relations between the parameters ruling each mechanism and the main spectral features, i.e., the peak position and the width of the acoustic mode, as well as the intensity and the width of the central quasielastic contribution. From the inset of Fig. 5, it can be seen that for the slow process the condition $\omega_l(Q)\tau_\alpha(Q) > 1$ always holds, so that this mechanism contributes mostly to the elastic linewidth rather than to the acoustic mode broadening. On the other hand, the fast microscopic process is such that $\omega_l(Q)\tau_\mu(Q) \leqslant 1$ at low Q, so that in this region it contributes to the acoustic damping. However, at wave vectors $Q > 5\ \mathrm{nm}^{-1}$, one reaches the crossover $\omega_l(Q)\tau_\mu(Q) \approx 1$, so that the fast mechanism drives an effective increase of the sound speed toward a limiting, solidlike, instantaneous response. As the weight of the fast process exceeds that of the slow one [namely $A(Q) \ll 1$ in Eq. (3), cf. Fig. 4], the increase of the sound speed basically stems only from the fast microscopic mechanism, which above the crossover threshold is also responsible for the broader tails of the quasielastic portion of the spectra ($\tau_\alpha \gg \tau_\mu$).

In Fig. 6, we report the *deconvoluted* spectra, i.e., the $S(Q,\omega)$ as obtained from the fitting procedure, together with the relative current correlation spectra $J(Q,\omega) = \omega^2/Q^2 S(Q,\omega)$. The latter quantity plays an important role in the description of the dynamical features of the system because its maxima are related to $c_l = \omega_l/Q$, namely the apparent sound speed of the system.

Finally, in Fig. 7, we compare the Q-dependent sound speed in liquid Al (calculated as the maximum of the fitting-

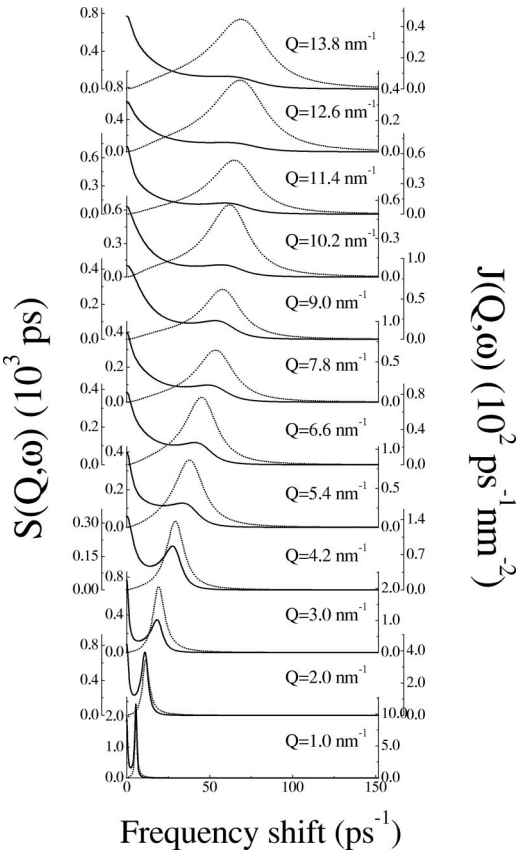

FIG. 6. Deconvoluted spectra of the density correlation function $S(Q,\omega)$ (left axis) and of the current correlation function $J(Q,\omega)$ (right axis) as obtained from the fit.

deconvoluted longitudinal current correlation function $[J(Q,\omega)=\omega^2/Q^2S(Q,\omega)]$ with the one previously determined in liquid lithium. Suitable reduced units (velocities normalized to their respective isothermal values, wave vectors measured in units Q_m) have been adopted.

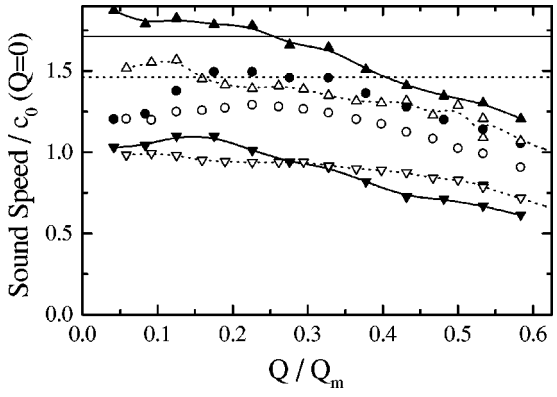

FIG. 7. Effective sound speed (dots) of aluminum (full symbols) vs lithium (open symbols). Data have been scaled by Q_m, the first sharp diffraction peak, and $c_0(0)$, the isothermal speed of sound in the hydrodynamic limit ($c_0^{\mathrm{Li}}=4450$ m/s; $c_0^{\mathrm{Al}}=4700$ m/s). $c_0(Q)$ is also reported (-▽-) together with the $c_\infty(Q)$ values determined by the fitting (-△-) and by the pair distribution function and interatomic potential (lines). The lines connecting the symbols are guidelines for the eyes only.

Both systems are seen to exhibit a clear positive dispersion effect, i.e., an increase of the sound speed at increasing the exchanged wave vector. Such dispersion, in ordinary liquids, proceeds between the adiabatic ($Q\rightarrow 0$) limit, $c_s=\sqrt{\gamma}c_0$, and the unrelaxed, instantaneous value, $c_\infty(Q)=\sqrt{\gamma\omega_0^2(Q)+\Delta^2(Q)}/Q$, where Δ^2 is the total strength of the nonthermal processes. In metallic liquids, instead, due to the high thermal conductivity, the condition $\omega_l(Q)<D_TQ^2$ holds for $Q\gtrapprox 0.1\,\mathrm{nm}^{-1}$, i.e., in the IXS Q window ($Q>1\,\mathrm{nm}^{-1}$), no region exists where the three relaxation processes—thermal, α, μ—are simultaneously unrelaxed. As a consequence, the lower and upper values of the sound speed are expected to be the isothermal $c_0(Q)$ [defined in Eq. (1)] and the partially unrelaxed $c'_\infty=\sqrt{\omega_0^2(Q)+\Delta_\alpha^2(Q)+\Delta_\mu^2(Q)}/Q$ [20].

To test the reliability of our model, we finally compared $c_\infty^{\mathrm{fit}}(Q)$ with the theoretical value $c_\infty^{\mathrm{th}}(0)$ deduced from the structure and interatomic potential data [17,21]. In both systems, the fitted values of $c_\infty^{\mathrm{fit}}(Q\rightarrow 0)$ slightly exceed the data for $c_\infty^{\mathrm{th}}(0)$ reported in the literature. A possible explanation of this inconsistency may be ascribed to the arbitrary choice of the memory function shape, which in principle can have more complicated features than the double exponential ansatz of Eq. (3). The major drawback of such an assumption is, indeed, the cusp at $t=0$. It is reasonable to think that an exponential decay forced to represent a more complicated time dependence can give an accurate estimate as far as the τ is concerned, while at short times the lack of a zero second derivative inescapably leads to an overestimate of $M_L(Q,t=0)$, the positive dispersion amplitude. A similar effect, i.e., the overestimation of the $c_\infty(Q)$ deduced by the fit, has also been observed in liquid lithium, where the same memory function has been adopted [14].

IV. CONCLUSION

In this work, the inelastic x-ray scattering technique has been utilized to study in detail the main features of the microscopic dynamics in liquid aluminum in the mesoscopic momentum region ($Q\approx 1-15\,\mathrm{nm}^{-1}$), i.e., the region in which the collective properties are dominant. Aluminum is a system where the investigation of the dynamics using the well-established inelastic neutron scattering technique is not possible. The present IXS experiments allowed for the determination of the pattern of relaxation processes entering in the density-density memory function, and therefore affecting the spectral shape of the dynamic structure factor. Specifically, the high quality of the data allows us to identify uniquivocally the presence of three distinct relaxation processes. The first one—the usual thermal relaxation—is associated with the coupling between density and energy fluctuations. As in alkali metals, although its relevance is rather small, this process cannot be neglected; more interesting, it plays a role that is different with respect to the ordinary nonconducting liquids. Much more important is the unambiguous evidence of *two well separated time scales* in the decay of that part of the memory function that is associated to the generalized viscosity. In particular, the present experiment proves that the tra-

ditional description of the generalized viscosity by a single time scale (viscoelastic model) cannot account for the detailed shape of $S(Q,\omega)$, and that it only provides a qualitative description of the microscopic dynamics in liquid metals.

The presence of two time-scale decays of the memory function poses a question of crucial importance: namely, what is their physical origin and, most important, which is the fast one?

The slow process, making use of the terminology used to describe glass-forming systems, is related to the α-relaxation that, in systems capable of sustaining strong supercooling, is responsible for the liquid-glass transition. From a more canonical point of view, this process can be framed within kinetic theory in terms of ''correlated collisions'': in mode-coupling approaches, the onset of these correlation effects is traced back to the coupling to slowly relaxing dynamical variables, and specifically in the liquid region to long-lasting density fluctuations. The quantitative description of this ''slow'' time scale requires a full evaluation of the mode-coupling contribution at different wave vectors, which is beyond the aim of the present work.

As far as the fast process is concerned, the situation is more confused and its interpretation is still a matter of debate. This is particularly annoying because—as shown in this paper for liquid aluminum and as demonstrated in the case of liquid lithium—the fast process is indeed more relevant than the slow one: it largely controls both the sound velocity dispersion and attenuation in the mesoscopic Q region. Historically, within a generalized kinetic theory approach, the fast initial decay of the density fluctuation memory function is traced back to collisional events, which are fast, short range, and, more important, uncorrelated among each others. Within this scheme, the short time scale τ_μ turns out to be associated with the duration of a rapid structural rearrangement occurring over a spatial range $\cong 2\pi/Q_m$. Although this description of the fast process in terms of uncorrelated interparticle collision is a possible way to qualitatively account for the dynamical features at short times in liquids and dense systems, it seems to be unable to account for similar results obtained in glasses [21–23], where the *collective* aspect of the dynamics cannot be neglected.

A possible, and different, approach to describe the initial fast decay of the memory function in dense fluids and liquids relies on the normal-mode (''instantaneous'' in normal liquids) analysis of the atomic dynamics [24], an approach that works correctly in the limiting case of ''harmonic glasses.'' In this case, one uses a framework (dynamical matrix, etc.) formally similar to the one customarily adopted for harmonic crystals; however, due to the lack of translational symmetry of the system, it turns out [22] that the eigenstates can no longer be represented by plane waves (PW's) even at relatively small wave vectors [25]. A scattering experiment, where Q is fixed, is equivalent—via the fluctuation-dissipation relation—to a response experiment, where one studies the time evolution of the system after a *sinusoidal* perturbation (with period $2\pi/Q$) is applied to the system itself. In the case of measuring the $S(Q,\omega)$, the applied perturbation is a density fluctuation. As the PW's are not eigenstates of the disordered systems, the initial perturbation can be projected along different eigenmodes, each one evolving in time with its own frequency. As a consequence of this frequency spread, the energy initially stored in the PW *relaxes* towards other PW's with different Q values. This process is exactly what one would expect in the presence of a relaxation process, and its characteristic time is determined by the projection of the system eigemodes on the PW basis (Fourier transform of the eigenvectors). We deal, therefore, with a mechanism whose ultimate origin is the topological disorder, and not a truly dynamical event. Ordinary liquids (such as the one considered here) are certainly ''disordered systems'' and at the high frequency considered here ($\omega\tau_\alpha \gg 1$) they can be considered as ''frozen''; therefore, the description used for glasses can be applied as well. Obviously, the ''harmonic approximation'' and the residual effect of the finite value of $\omega\tau$ prevent the ''quantitative'' application of the previously described formalism to the case of normal liquids. However, we expect that—on a qualitative basis—the fast relaxation process in liquids can be described in term of ''high-frequency vibrations'' (that are a strongly correlated atomic motion), and this point of view appears to be in contrast with the (uncorrelated) binary collision based description.

At the present stage, the experimental data cannot support either interpretation. However, the possibility that the phenomenology reported here for a simple liquid can be understood within the same mental framework developed for more complex liquids and glasses is certainly appealing.

[1] J. R. D. Copley and M. Rowe, Phys. Rev. A **9**, 1656 (1974).
[2] T. Bodensteiner, Chr. Morkel, W. Gläser, and B. Dorner, Phys. Rev. A **45**, 5709 (1992).
[3] C. Morkel and W. Glaser, Phys. Rev. A **33**, 3383 (1986); A. Stangl, C. Morkel, U. Balucani, and A. Torcini, J. Non-Cryst. Solids **205–207**, 402 (1996).
[4] P. Verkerk, P. H. K. De Jong, M. Arai, S. M. Bennington, W. S. Howells, and A. D. Taylor, Physica B **180&181**, 834 (1992).
[5] A. G. Novikov, V. V. Savostin, A. L. Shimkevich, R. M. Yulmetyev, and T. R. Yulmetyev, Physica B **228**, 312 (1996).
[6] P. Chieux, J. Dupuy-Philon, J. F. Jal, and J. B. Suck, J. Non-Cryst. Solids **205–207**, 370 (1996).
[7] H. Mori, Prog. Theor. Phys. **33**, 423 (1965).
[8] D. Levesque, J. Verlet, and J. Kurkijarvi, Phys. Rev. A **7**, 1690 (1973).
[9] J. Casas, D. J. Gonzales, and L. E. Gonzales, Phys. Rev. B **60**, 10 094 (1999); J. Casas, D. J. Gonzales, L. E. Gonzales, and M. Silbert, J. Non-Cryst. Solids **250-252**, 102 (1999).
[10] U. Balucani and M. Zoppi, *Dynamics of the Liquid State* (Clarendon Press, Oxford, 1994).
[11] T. Scopigno, U. Balucani, A. Cunsolo, G. Ruocco, F. Sette, and R. Verbeni, Europhys. Lett. **50**, 189 (2000); e-print cond-mat/9911021 (unpublished).

[12] J. P. Boon and S. Yip, *Molecular Hydrodynamics* (McGraw-Hill, New York, 1980).
[13] T. Scopigno, U. Balucani, G. Ruocco, and F. Sette, Phys. Rev. Lett. **85**, 4076 (2000).
[14] T. Scopigno, U. Balucani, G. Ruocco, and F. Sette, J. Phys.: Condens. Matter **12**, 8009 (2000); e-print cond-mat/0001190 (unpublished).
[15] M. M. G. Alemany, J. Casas, C. Rey, L. E. Gonzales, and L. J. Gallego, Phys. Rev. E **56**, 6818 (1997).
[16] W. Gudowski, M. Dzugutov, and K. E. Larsson, Phys. Rev. E **47**, 1693 (1993).
[17] T. Gaskell, J. Phys. F: Met. Phys. **16**, 381 (1986); Phys. Chem. Liq. **17**, 11 (1987).
[18] I. Ebbsjo, T. Kinnel, and I. Waller, J. Phys. C **13**, 1865 (1980).
[19] O. J. Eder, B. Kunsch, J. B. Suck, and M. Suda, J. Phys. (Paris), Colloq. **41**, C8-226 (1980).
[20] By a numerical point of view, the difference between $c_\infty(Q)$ and $c'_\infty(Q)$ is of the order of $\sqrt{\gamma}$ (3%), namely, within the statistical errors of the fitting procedure. It is worth pointing out how the thermal process, contrary to what happens in ordinary liquids, gives also a nonviscous damping $\delta\omega=(\gamma-1)c_0^2(Q)/D_T$, responsible for an additional Brillouin linewidth that is particularly important at the lower Q's of our experiment.
[21] T. Scopigno *et al.* (unpublished).
[22] G. Ruocco, F. Sette, R. Di Leonardo, G. Monaco, M. Sampoli, T. Scopigno, and G. Viliani, Phys. Rev. Lett. **84**, 5788 (2000).
[23] W. Gotze and M. R. Mayr, Phys. Rev. E **61**, 587 (2000).
[24] G. Seeley and T. Keyes, J. Chem. Phys. **91**, 5581 (1989).
[25] V. Mazzacurati, G. Ruocco, and M. Sampoli, Europhys. Lett. **34**, 681 (1996).